Title
RECOIL PROPERTIES OF FISSION PRODUCTS

Authors
Alexander, John M.
Gallagher, M. Frances.

Publication Date
1959-12-01

UCRL-8978

UNIVERSITY OF CALIFORNIA

Ernest O. Lawrence Radiation Laboratory

BERKELEY, CALIFORNIA

DISCLAIMER

UCRL-8978

UNIVERSITY OF CALIFORNIA

Lawrence Radiation Laboratory
Berkeley, California

Contract No. W-7405-eng-48

RECOIL PROPERTIES OF FISSION PRODUCTS

John M. Alexander and M. Frances Gallagher

December 1959

Printed for the U. S. Atomic Energy Commission

RECOIL PROPERTIES OF FISSION PRODUCTS

John M. Alexander and M. Frances Gallagher

Lawrence Radiation Laboratory
University of California
Berkeley, California

December 1959

ABSTRACT

Radiochemical measurements have been made of the range of five fission products in Al and Au. The relative rates of energy loss in Au and Al were also measured radiochemically. Range-energy curves for the median light product of fission and the median heavy product have been constructed from these measurements and the energy-loss data of others. The relation of range (R) to energy (E) or velocity (V) can be fitted to functions of the form $R = kV^{-\Delta}$ or $R = KE^{2/3}$. We have assumed that these functional forms can be applied to fission products of any mass. The total range and original energy measurements have been used to determine the constants K and Δ for the products of high yield. These constants have been extrapolated to products of low yield, and the measured ranges have been used to estimate kinetic energies.

We have interpreted certain radiochemical observations in terms of a scattering parameter q, the average range perpendicular to the original velocity. The value of q in Au has been estimated to be about one-fourth the total range.

RECOIL PROPERTIES OF FISSION PRODUCTS*

John M. Alexander and M. Frances Gallagher

Lawrence Radiation Laboratory
University of California
Berkeley, California

December 1959

INTRODUCTION

Many experiments have been directed toward the study of the fission process by observation of the recoil properties of the fission products.[1-11] The interpretation of the experimental observations always involves certain assumptions concerning stopping phenomena, namely the relationship of range to energy and the deviations from straight-line motion. The experimental information concerning these aspects of the stopping process is somewhat fragmentary. This paper presents some new radiochemical observations and discusses them along with existing experimental measurements of range, energy, energy loss, and range of fission products.

Several different techniques have been used for the observation of the recoils. Measurements of the range,[11] energy,[12] the rate of energy loss,[13,14] and the angular distribution[5-10] of the fission products have been made with well-collimated recoils. On the other hand, measurements with poorly collimated recoils have been made of the range,[1-4,15,16] the velocity of the fissile nucleus,[2-4] and certain features of the angular distribution.[3] The experiments employing good collimation are limited by sensitivity considerations to very intense sources of fission or gross fission-product studies. The experiments using poor angular resolution have much higher sensitivity but must be analyzed

*Work under the auspices of the U.S. Atomic Energy Commission.

by means of integrations over the appropriate angles involved.[17] Meaningful results from these integrations require a knowledge of (a) the range-energy relationship, (b) the deviations from straight-line motion, and (c) the form of the angular distribution.

In this study, the radiochemical method has been used to measure three properties of stopping phenomena: (a) the average range of the products, (b) the relative rates of energy loss in two materials, and (c) the average ratio of range perpendicular to the original velocity to the total range. Specifically, the ranges have been measured in Al and Au for five products from thermal-neutron-induced fission of U^{235}. From these and other measurements,[15,16] curves of range as a function of mass number have been constructed. These curves define quite accurately the ranges of the median light and heavy products. (By "median product" is meant that fragment that is the median of all the light fission products or all the heavy fission products.) Energy-loss data[13,14] are available for median light and heavy products, and we have normalized them to the range measurements. The range-energy curves are given for median light and heavy products. Similar range-energy curves are proposed for all fission products.

EXPERIMENTAL PROCEDURE

Radiochemical measurements of the range of Sr^{89}, Ag^{111}, Cd^{115}, I^{131}, and Ba^{140} from thermal-neutron fission of U^{235} have been made by the low-angular-resolution technique originated by Douthett and Templeton.[1] The target diagram is shown in Fig. 1. A thin layer of U^{235} was sprayed on 0.00025-in. Al foil,[18] and its thickness was determined by a measurement of the alpha radiation per

unit area. The target and several catcher foils (see Fig. 1) were stacked one on top of the other, and clamped between two pieces of cardboard. The target assembly was irradiated in the thermal column of the LPTR reactor at Livermore for several days with a flux of ~5 x 10^{11} neutrons/cm^2 sec.

Commercially rolled Al foils (99.5% Al) were wiped with a lint-free tissue and cut into squares of 10.26 cm^2 with a stainless steel template. A very smooth central region of about 36 in^2 was found for all Al sheets. All squares cut from this central region of a given Al sheet had weights uniform within at least 0.5%. Commercially available Au foil was not so uniform, and thus more uniform Au foils were prepared by evaporation. The thickness of the foils other than 1A and 1B is not so critical for the range measurement, and the commercial Au foil was used for those catchers.

After irradiation, the foils were separated and dissolved in HCl and H_2O_2. The target layer was included with the catcher designated 1A. Iodine carrier was always present during the dissolution if iodine was to be separated. Standard radiochemical procedures were used.[19] Chemical yields were determined by weighing before counting and checked by another analysis after counting. These two analyses had an average deviation of about 1%. Counting was done with β proportional counters or with an integral γ counter. All samples of the same element from a given experiment were counted on the several β counters used, in rotating fashion, in order to minimize counting-efficiency effects. The chemical yields were so similar (usually constant to 10%) that counting-efficiency corrections were in general negligible. The γ radiation from I^{131} and Ba^{140} was also counted on a NaI scintillation detector sensitive to all photons with energy greater than about 60,000 electron volts.

Table I

Experiments with Al catchers
Fraction of activity observed for the various catchers

Fission product	Expt. no.	Catchers Number, substance, thickness (mg/cm^2) 3A Al 1.92	2A Al 1.92	1A+tgt. Al 1.923	1B Al 1.923	2B Al 1.92	3B Al 1.92	Target thickness (mg/cm^2)U^{235}
Sr^{91}	1	.0264	.2287	.2501	.2396	.2318	.0234	.062
Sr^{89}	2	.0215	.2378	.2400	.2414	a	a	.122
Ag^{111}	3		.2264	.2816	.2739	.2181		.045
Ag^{111}	2		.2083	.2908	.2873	.2136		.122
Ag^{111}	4		.1882	.3258	.2971	.1888		.368
I^{131}	3		.2099	.2849	.2915	.2139		.045
I^{131}	2		.1990	.3060	.2983	.1967		.122
I^{131}	4		.1779	.3344	.3128	.1750		.368
Ba^{140}	1		.1703	.3349	.3284	.1665		.062
Ba^{140}	2		.1602	.3437	.3342	.1617		.122

[a]These samples were lost, therefore the total activity was obtained with the assumption that 2A+3A = 2B+3B.

Table II

Experiments with Au and Al catchers
Fraction of activity observed in the various catchers

Catcher, thickness (mg/cm^2), substance

Experiment 5

Fission product	3A 1.626 Al	2A 1.626 Al	1A+tgt. 1.626 Al	1B[a] 4.876 Au	2B 1.056 Al	3B 1.036 Al	4B 1.002 Al	Target[b] 0.035 U^{235}	F_b[c] Fraction backscattered
Sr^{89}	.1020	.2110	.2258	.1645	.1466	.1278	.0224	.0062	.0357
Ag^{111} d	.0384	.2263	.2662		.1444	.0973	<.002	.0073	.0272
Cd^{115} d	.0200	.2320	.2715		.1518	.0787	<.002	.0077	.0196
I^{131} d	.0218	.2331	.2824		.1559	.0834	<.002	.0076	.0335
Ba^{140}	<.002	.2261	.3074	.2556	.1611	.0496	<.0004	.0086	.0292

Experiment 6

Fission product	3A 1.626 Al	2A 1.626 Al	1A+tgt. 1.626 Al	1B 4.953 Au	2B 1.053 Al	3B 1.044 Al	4B 1.031 Al	Target 0.017 U^{235}	F_b Fraction backscattered
Sr^{89}	.1026	.2008	.2301	.1700	.1463	.1300	.0203	.0030	.0320
Ag^{111} d	.0377	.2288	.2633		.1483	.0989	e	.0035	.0281
I^{131} d	.0213	.2355	.2834		.1524	.0837	<.0004	.0037	.0385
Ba^{140}	<.0006	.2250	.3117	.2583	.1588	.0462	<.0001	.0042	.0346

Experiment 7

Fission product	3A 1.628 Al	2A 1.628 Al	1A+tgt. 1.625 Al	1B plus 1.986 Au	2B 1.650 Al	3B 1.650 Al	Target .011 U^{235}	F_b Fraction backscattered
Sr^{89}	.1032	.1940	.2209	.2778		.2042	.0020	.0171
Cd^{115}	.0211	.2321	.2785	.3398		.1285	.0024	.0305
Ba^{140}	.0024	.2233	.3023	.3698		.1021	.0027	.0266

Experiment 8

Fission product	3A 4.622 Au	2A 4.717 Au	1A+tgt. 1.626 Al	1B 4.971 Au	2B 4.970 Au	3B 4.758 Au	Target .015 U^{235}	F_b Fraction backscattered
Ba^{140}	.0055	.2147	.3135	.2690	.1961	.0013	.0037	.0319

[a] The Au foil was prepared by evaporation, its uniformity checked by cutting small squares from various parts of the foil. Activation of impurities in the Au was checked in Experiments 7 and 8, and found to be negligible.

[b] The activity retained in the target was taken to be $\left(\frac{k_{Al}}{k_W}\frac{W}{2R_{Al}}\right)$ from the data in Table V. The results are not very sensitive to this correction because the targets were quite thin.

Table II (cont'd.)

[c] The fraction of the total activity in the A foils in excess of one half was attributed to backscattering from the Au. The quantity (F_b) is defined as the net fraction backscattered. F_b was determined by adding the fractions in the A foils, subtracting one-half the calculated fraction in the target, and comparing with 0.5000.

[d] No observation was made of 1B in these cases. The total activity was calculated from the activity observed in catchers 2A+3A and the average range value reported in Table V (Eq. (6)).

[e] Some activity of long half life was observed in this foil, which prevented setting a limit on the Ag^{111} activity.

The experimental observations are presented in Tables I and II. Column 1 gives the fission product studied. Columns 3-8 in Table I and 2-8 in Table II give the designation (see Fig. 1) of each catcher foil, its thickness and type, and the fraction of the total atoms in question that stopped in that foil. The last column in Table I gives the target thickness. Column 9 of Table II gives the estimated fraction of the activity retained by the target. The excess activity observed in the A foils (greater than 1/2 the total plus 1/2 column 9) is attributed to backscattering and is given in the final column of Table II.

ANALYSIS

The equations used to analyze the experimental observations are presented in this section. A list of the symbols is given in the Appendix. First we derive a simple relationship, Eq. (6), for calculating the range from experiments in which the catcher foils are of the same material. Then we consider the situation in which catcher foils of different materials are used. The different scattering properties of the two materials are included in the derivation of Eqs. (13) and (14). Finally we discuss the measurement of relative stopping powers of two materials.

For fission induced by thermal neutron irradiation the fissile nucleus is essentially at rest and the angular distribution is isotropic. Thus F_t, the fraction of the activity from a target of thickness W that passes through a catcher of thickness t, is given as

$$F_t = \frac{1}{4\pi W} \int_0^W dx \int_0^{\theta_{max}} 2\pi \sin\theta d\theta. \qquad (1)$$

The symbol x denotes the distance in the fissile target layer of the fission event from the surface of the catcher in question. The angle θ is defined by the normal to the target layer and the direction of recoil. The limit of integration θ_{max} is determined by the residual range R' of the product as it emerges from the target layer (see Fig. 2A):

$$\cos\theta_{max} = t/R'. \qquad (2)$$

If the target layer is thin with respect to the range of the product, we may approximate the rate of velocity loss $\frac{dV}{dx}$ in the target layer as a constant, $\frac{1}{k}$:

$$\frac{dV}{dx} = \frac{1}{k} , \tag{3}$$

or

$$R_i = k_i V - \Delta_i , \tag{4}$$

where Δ_i is a constant.

$$\text{Then } \cos \Theta_{max} = \frac{t}{k_i \left[V - \frac{1}{k_W} \frac{x}{\cos \Theta_{max}} \right] - \Delta_i} \cong \frac{t}{R_i} + \frac{x}{R_i} \left(\frac{k_i}{k_W} \right) \tag{5}$$

$$\text{and} \quad F_t = \frac{1}{2} \left(1 - \frac{t}{R_i} - \frac{W}{2R_i} \frac{k_i}{k_W} \right) = \frac{1}{2} \left(1 - \frac{t'}{R_i} \right) , \tag{6}$$

$$\text{where } t' = t + \frac{W}{2} \frac{k_i}{k_W} . \tag{7}$$

The subscripts i and W refer to catcher and target materials, $1/R$ is the average reciprocal range of the product, and t' is the effective thickness of the catcher and target (to first order in W/R_W). The approximation has been made that dV/dx is constant for the fragments while in the target layer. This is possibly not a good approximation for those recoils which are appreciably slowed down in the target, therefore only F_t values with $t \gg W(k_i/k_W)$ should be used to deduce range values. The implicit assumptions have been made that the recoiling atom moves in a straight line and that $R_i - t - W(k_i/k_W)$ is much greater than the range straggling.

Bohr has presented a qualitative theory of the stopping of fission fragments.[20] The theory predicts that nuclear collisions will provide the major mechanism of energy loss at the end of the range, whereas the initial degradation is mainly by ionization. In the ionization region very small angular deflections and small range straggling are expected. However, in the nuclear-stopping region, larger deflections and the major contribution to the range straggling are

expected. Fission-fragment tracks in photographic emulsions[21] and cloud chambers[22] bear out the theory with respect to angular deflections. The experimental measurements of range straggling also agree with these theoretical expectations.[11,20] The recoiling product is thus expected to move straight initially and to suffer deflections as it approaches the end of the range, as shown in Fig. 2B. Let us define the vectors $\vec{p}$ as the average component of range along the original direction of motion and $\vec{q}$ as the average component of the range perpendicular to the original direction of motion. Then we have

$$\vec{R} = \vec{p} + \vec{q} , \tag{8}$$

$$R = (p^2 + q^2)^{1/2} = p[1 + (q/p)^2]^{1/2}. \tag{9}$$

It is clear that the foregoing analysis did not take account of the angular deflection. This effect can be included by allowing $\vec{q}$ to be equally probable at all azimuthal angles φ measured with respect to the plane of $\vec{p}$ and the normal to the target layer (X, Z plane in Fig. 2B).

Let us consider an infinitely thin target layer on the YZ plane, and let θ be the angle between $\vec{p}$ and the normal to the YZ plane. Then for the fraction F_b' of the recoils that backscatter from one catcher foil we have $\theta < \pi/2$ but final values of x are negative:

$$F_b' = \frac{1}{4\pi} \int_{-\pi/2}^{\pi/2} d\varphi \int_{\pi/2}^{\theta_{min}} \sin \theta d\theta, \tag{10}$$

where

$$p \cos \theta_{min} = q \cos \varphi \sin \theta_{min}; \tag{11}$$

after integration,

$$F_b' = \frac{1}{2\pi} \arcsin \left(\frac{q}{R}\right) \cong \frac{1}{2\pi} \frac{q}{R} . \tag{12}$$

If the catching materials are identical on either side of the target layer, then the net fraction backscattered F_b is zero, but if the materials differ as

designated by subscripts, then

$$F_b \cong \frac{1}{2\pi}\left[\left(\frac{q}{R}\right)_i - \left(\frac{q}{R}\right)_j\right]. \qquad (13)$$

If we assume that the range-energy relationships in materials i and j are simply proportional to each other, we can derive a relationship for the fraction of the activity ($_jF_i$) that passes through a thickness of t_i of material i ($t > q_i$) into a catcher of material j.

$$ {}_jF_i = \frac{1}{2} - \frac{1}{2}\left(\frac{t}{p}\right)_i + \frac{1}{2\pi}\left\{\text{arc sin}\left[\frac{q}{(R^2-t^2)^{1/2}}\right]_i - \text{arc sin}\left[\frac{q_j}{(1-t_i^2/R_i^2)^{1/2}R_j}\right] - \right.$$

$$\left. \text{arc sin}\left[\frac{t\ q}{p(R^2-t^2)^{1/2}}\right]_i + \text{arc sin}\left[\frac{t_i\ q_j}{p_j(R_i^2-t_i^2)^{1/2}}\right]\right\} + \frac{1}{4}\left[\frac{t}{p} - \frac{t}{R}\right]_i + \frac{1}{4}\frac{R_j}{R_i}\left[\frac{t_i}{p_j} - \frac{t_i}{R_j}\right]$$

$$ {}_jF_i \cong \frac{1}{2} - \frac{1}{2}\left(\frac{t}{p}\right)_i + F_b\left[1 - \frac{1}{2}\left(\frac{t}{R}\right)_i^2 - \frac{1}{8}\left(\frac{t}{R}\right)_i^4\right] + \frac{1}{8}\left(\frac{t}{p}\right)_i\left[\left(\frac{q}{R}\right)_i^2 + \left(\frac{q}{R}\right)_j^2\right] \qquad (14)$$

For the special case of the same stopping materials i and j, Eq. (14) reduces to Eq. (6).

The values of $\left(\frac{q}{R}\right)$ derived from Eq. (13) do not require the assumption that the recoil path coincides with $\vec{p}$ and $\vec{q}$. Only the effect of recoils crossing the interface more than once has been ignored. However, Eq. (14) depends on the assumption that the recoil path coincides with $\vec{p}$ and $\vec{q}$ on the average. The error due to this approximation is not expected to be large, but is difficult to evaluate quantitatively.

Information can be obtained concerning relative rates of energy loss if a measurement is made of the fraction of activity F_{i+j} penetrating the combined foils t_i of material i and t_j of material j,

$$F_{i+j} = \frac{1}{2}(1 - \cos \theta_{max}). \qquad (15)$$

The θ_{max} value derived from this measurement of F_{i+j} represents the angle made by a fission product which penetrates a thickness $\frac{t_i}{\cos \theta_{max}} \equiv T_i$ of material i and has a residual range in substance j of $t_j/\cos \theta_{max} \equiv RR_j$. Thus this measurement combined with the total range measurement specifies a fractional range loss $\left(\frac{T_i}{R_i}\right)$ in substance i and a fractional residual range $\left(\frac{RR_j}{R_j}\right)$ in substance j. If these quantities sum to unity, the range-energy relationships in the two substances are simply proportional to each other (for the particular values of T_i and RR_j observed). If the sum is greater than unity the ratio of the initial fractional energy loss $\left(\frac{\Delta E}{E}\right)$ to the initial fractional range loss $\left(\frac{\Delta R}{R}\right)$ is less in the first material than in the second. This is quite a simple and accurate way of measuring the relative stopping power of various materials.

Appendix: Symbols Used

F_t: The fraction of the total activity of a specific nuclide that passes through catcher foils of combined thickness t (all catcher foils of the same material).

W: The thickness of the fissile layer.

x: The distance of a particular fission event from the surface of the fissile layer.

θ: The angle between the normal to the target layer (see Fig. 2) and the original recoil direction. The subscripts max and min designate maximum and minimum values of θ in the various integrations.

R': The residual range of a fission product as it emerges from the target layer and enters the first catcher foil.

V: The speed of a fission product.

E: The kinetic energy of a fission product.

R_i (e.g., R_{Al}): The range of a given fission product in the stopping material designated by the subscript. Subscripts refer to materials used as catcher foils, and the subscript W refers to the target layer.

k_i, Δ_i, K_i, and α_i: Constants for a given fission product and stopping material i in the equations $R_i = k_i V - \Delta_i$ and $R_i = K_i E^{\alpha_i}$.

t': The effective thickness of catcher foils and target layer corrected to first order in W/R_W.

p: The average component of the range of a fission product parallel to its original direction of motion.

q: The average component of the range of a fission product perpendicular to its original direction of motion.

φ: The angle between the direction of q and the plane of p and the normal to the target layer (see Fig. 2B).

F_b': The fraction of the atoms that recoil into a catcher foil but backscatter out of the foil, e.g., have $\theta < \pi/2$ but final values of X that are negative (see Fig. 2B).

F_b: The difference between the fractions gained and lost by backscattering (see Eq. (13)).

${}_jF_i$ (e.g., ${}_{Al}F_{Au}$): The fraction of the total activity of a specific nuclide that passes through a thickness t_i of material i into a catcher of material j.

F_{i+j} (e.g., F_{Au+Al}): The fraction of the total activity of a specific nuclide which penetrates a thickness t_i of material i followed by t_j of material j.

T_i and RR_j: A fission product is completely stopped by a thickness T_i of material i followed by a thickness RR_j of material j. In other words, after traversing a thickness T_i of material i, the fission product has a residual range RR_j in material j.

TREATMENT OF EXPERIMENTAL DATA

In Table III the various range values are given for the experiments using only Al catcher foils. From Eq. (6) it is clear that

$$\left(\frac{\partial F_t}{\partial W}\right)_t = \frac{k_i}{k_W} \quad \frac{W}{4R_i}$$

The value of $\left(\frac{\partial F_t}{\partial W}\right)_t$ was determined by a least-squares fit to the data of Table I (see Fig. 3). The $\frac{k_{Al}}{k_W}$ was evaluated by successive approximations. This correction factor was used in all subsequent experiments to evaluate the effective thickness t' (Eq. (7)), which was used in place of t in Eq. (14). The magnitude of k_{Al}/k_W can be estimated with the crude assumption that $k_i/A_i^{1/2}$ is a constant, and by taking the composition of the target layer to be U_3O_8. The k_{Al}/k_W value of 1.47 found in these experiments is greater than estimated. A similar effect was observed by Douthett and Templeton, who suggested that inhomogeneities in the target layer might increase the effective target thickness.

The results of the analysis of the experiments using Al and Au catcher foils are given in Table IV. The first two columns give the particular fission product and experiment. Column 3 presents the value of the range in Al, and column 6 the range in Au. The measured quantity $(q/R)_{Au} - (q/R)_{Al}$ is

Table III

Results of experiments with Al catchers.
Range values (mg/cm^2 Al) calculated from the F_t values observed in various catchers[a]

Fission product	Catchers				Experiment number
	3A	2A+3A	2B+3B	3B	
Sr^{91}	$\lesssim$4.11[b]	4.02	4.02	$\lesssim$4.08[b]	1
Sr^{89}	$\lesssim$4.11[b]	4.18			2
Ag^{111}		3.57	3.47		3
Ag^{111}		3.45	3.51		2
Ag^{111}		3.52	3.52		4
I^{131}		3.37	3.42		3
I^{131}		3.34	3.32		2
I^{131}		3.40	3.37		4
Ba^{140}		2.99	2.95		1
Ba^{140}		2.96	2.98		2

[a] These values were calculated from Eq. (5),

$$R = \frac{t + \frac{k_{Al}}{k_W}\frac{W}{2}}{1 - 2F_t},$$

taking $k_{Al}/k_W = 1.47$ for all cases.

[b] The values from catchers 3A and 3B of Experiment 1 were omitted because of possible violation of the straggling requirement. In Experiment 2 experimental errors were evidently greater than the straggling perturbation.

Table IV

Results of experiments with Al and Au catchers

Fission product	Experiment number	R_{Al} (mg/cm^2)	$\left(\frac{q}{R}\right)_{Au} - \left(\frac{q}{R}\right)_{Al}$	$\left(\frac{q}{R}\right)_{Au}$ [c]	R_{Au} [d] (mg/cm^2)	T_{Au} (mg/cm^2)	$\frac{T_{Au}}{R_{Au}}$	RR_{Al} (mg/cm^2)	$\frac{RR_{Al}}{R_{Al}}$
Sr^{89}	5	4.12[a]	0.22	0.28	10.82	7.08	0.652	1.51	0.366
Sr^{89}	6	4.11[a]	0.20	0.25	10.89	7.14	0.657	1.51	0.366
Sr^{89}	7	4.11[a]				3.40	0.313	2.79	0.677
Ag^{111}	5		0.17	0.21	8.91	6.15	0.681	1.31	0.373
Ag^{111}	6		0.18	0.23	9.15	6.22	0.689	1.31	0.373
Cd^{115}	5	3.36[b]	0.12	0.15	8.61	5.88	0.683	1.25	0.375
Cd^{115}	7	3.31	0.19	0.24		2.71	0.315	2.22	0.667
I^{131}	5		0.21	0.26	8.69	5.95	0.685	1.27	0.377
I^{131}	6		0.24	0.30	8.66	5.99	0.690	1.26	0.374
Ba^{140}	5	3.01	0.18	0.23	8.00	5.50	0.683	1.17	0.393
Ba^{140}	6	2.98	0.22	0.28	7.92	5.50	0.683	1.16	0.389
Ba^{140}	7	2.98	0.17	0.21		2.53	0.314	2.07	0.695
Ba^{140}	8		0.20	0.25	8.23				

[a] These values were calculated from the fraction of activity observed in 3A (see Table II). Ranges for Sr^{89} calculated from the fraction in 2A were ~3% smaller; this is attributed to backscattered recoils. This effect is assumed to be negligible for the other products.

[b] This value was calculated from the ratio of fraction in 3A to the fraction in 2A relative to I^{131}. Straggling effects were assumed to be identical.

[c] We have assumed $\left(\frac{q}{R}\right)_{Au} = 5\left(\frac{q}{R}\right)_{Al}$.

[d] The scattering correction was made (see Eq. (14)) by using the average value of F_b and the arbitrary assumption $\left(\frac{q}{R}\right)_{Au} = 5\left(\frac{q}{R}\right)_{Al}$.

UCRL-8978

given in the fourth column. From the values in column 4 we have estimated $(q/R)_{Au}$ the scattering effect in Au, and these values are listed in column 5. In making this estimation we have assumed that $(q/R)_{Au} = 5\ (q/R)_{Al}$. The last four columns present the quantities related to relative rates of energy loss in Al and Au.

The values of $\left| (q/R)_{Au} - (q/R)_{Al} \right|$ evaluated from Eq. (13) and the measured quantity F_b were larger than expected. In addition to the F_b values from Experiments 5 and 6 there are two other experimental observations consistent with large values of $(q/R)_{Au}$. The first is the F_b value of 0.017, observed for Sr^{89} in Experiment 7, compared with 0.034 in Experiments 5 and 6. The thickness of the Au catcher (1B) in Experiment 7 was less than q_{Au} for Sr^{89}, which was estimated from Eq. (13), and Experiments 5 and 6. Thus the limits of integration in Eq. (10) should be altered, and a lower F_b is expected for Sr^{89} in Experiment 7. Secondly, the activity of Sr^{89} observed in catcher 2A of Experiments 5, 6 and 7 is slightly greater than that expected from the range deduced from all the other observations. This is believed to be due to a very small contribution from recoils scattered in the Au catcher (1B) which have enough energy to penetrate catcher 1A.

In a completely different experimental arrangement Coffin and Halpern have observed a group of recoiling fission products with about one-fifth the usual range.[8] They interpreted this observation as due to recoiling products scattered in their target layer. This result also indicates that large angular deflections are important in the stopping process, and, in fact, suggests a value of about one-fifth for (q/R).

Correction terms in Eq. (14), due to the magnitude of $(q/R)_{Au} - (q/R)_{Al}$, are fairly large. Thus the range values in Au from Experiments 5 and 6 are sensitive to the approximations made in the derivation of Eq. (14). It is very difficult to assign errors due to these corrections (as discussed in the preceding section), but we do not expect errors of more than ~2% for the range in Au. The agreement of the range of Ba^{140} in Experiments 5 and 6 with that from Experiment 7 bears out this guess. The calculation of residual ranges in Al after degradation in Au (T_{Au} and RR_{Al}) is independent of the scattering effect, provided that q is less than the thickness of the Al catcher, 2B.

The average range values determined in this work are given in Table V. The number of products measured in this study and in earlier experiments elsewhere is certainly very incomplete. However, it is possible to construct a somewhat fragmentary range-mass curve. The relative range values reported in Reference 16 are much more accurate than the absolute values. We have thus normalized those measurements to ours and have drawn a smooth curve in Fig. 4. This curve allows a fairly accurate interpolation to mass numbers near those of the products studied in this work. We consider that the range of the median-light and heavy fission products can be taken from this curve with an accuracy of $\lesssim$1.5%.

The ratio of range in Al to range in Au appears to be slightly dependent on the mass of the product as shown in Fig. 5.

Table V

Average range values

Fission product	Range in Al (mg/cm^2)	Range in Au (mg/cm^2)	R_{Al}/R_{Au}
Sr^{89}	4.12±0.02[a]	10.86±0.04[a]	0.379
Sr^{91}	4.02		
Ag^{111}	3.51±0.02	9.03±0.12	0.389
Cd^{115}	3.33±0.04	8.61	0.387
I^{131}	3.37±0.02	8.68±0.02	0.388
Ba^{140}	2.98±0.01	8.05±0.1	0.370

[a] The quoted errors are the standard deviation of the mean, $(SDM)^2 = \Sigma \frac{d^2}{(n-1)^2}$; the number of independent range measurements is somewhat less than n. The ranges in Au probably have additional systematic errors of ~2% because of the correction terms due to scattering.

RANGE-ENERGY CURVES

Energy-loss measurements[13,14] have been made for the median light and median heavy fission products. The masses of the median light and median heavy products (94.7 and 138.8) were obtained from the relationships $V_H/V_L = M_L/M_H$ and $M_L + M_H = 233.5$. Total ranges for products of these masses were taken from the smooth curves shown in Figs. 4 and 5. Also the corresponding ranges in air can be obtained from Reference 11. The range values in air must be corrected for the small difference in kinetic energy[12] of the products from the fission of Pu^{239} and U^{235}.

The energy-loss measurements have been normalized to the total range values, and the results are summarized in Table VI and Figs. 6-10. The first two columns in Table VI give the energy and corresponding velocity of the median light and heavy products; the next two columns the absorber thickness and corresponding range. Figures 6-8 show the range in Al, air, and Au as a function of velocity. Figure 6 also shows that the range-energy information for Al from Table VI is consistent with measurements of another type, the range of Tb^{149} from nuclear reactions induced by heavy ions.[23] For Al and air an equation of the form

$$R_i = k_i V - \Delta_i \qquad (16)$$

can fit the results accurately over quite a wide range. For Au this equation appears to give a fit which is more limited, but the data scatter considerably.

Figures 9 and 10 show $\log R_i$ plotted as a function of $\log E$. The smooth curves were simply drawn by eye to show that an equation of the form

$$R_i = K_i E^{\alpha_i} \qquad (17)$$

Table VI

Range-energy data for median light and median heavy fission products

Median light product, A = 94.7					Median heavy product, A = 138.8				
Energy (Mev)	Velocity $(Mev/A)^{1/2}$	Absorber (mg/cm^2)	Residual range (mg/cm^2)	Ref.	Energy (Mev)	Velocity $(Mev/A)^{1/2}$	Absorber (mg/cm^2)	Residual range (mg/cm^2)	Ref.
			Aluminum						
98.7	1.444	0	4.00	a,b	67.5	0.986	0	3.03	a,b
59.8	1.124	1.06	2.94	b	30.0	0.658	1.06	1.97	b
40.4	0.924	1.82	2.18	b	17.6	0.504	1.82	1.21	b
22.3	0.687	2.5	1.5	b					
96		0		c	65.6		0		c
			Gold						
98.7	1.444	0	10.54	a,b	67.5	0.986	0	8.13	a,b
62.0	1.144	3.29	7.25	b	33.5	0.695	3.29	4.84	b
37.4	0.889	5.09	5.45	b	19.2	0.526	5.09	3.04	b
79.	1.29	0.61	9.93	d	57.5	0.91	0.61	7.52	d
57.	1.10	2.20	8.34	d	38.5	0.74	2.20	5.93	d
41.	0.93	3.80	6.74	d	27.5	0.63	3.80	4.33	d
17.	0.60	8.35	2.19	d	36.0	0.72	2.54	5.59	e
53.2	1.06	3.30	7.24	e	15.3	0.47	5.54	2.59	e
21.9	0.68	6.96	3.58	e					
6.13	0.36	9.56	0.98	f					
			Air						
98.7	1.444	0	3.02	g,d	67.5	0.986	0	2.29	g,d
93.2	1.40	0.142	2.88	d	60.5	0.93	0.142	2.15	d
84.8	1.34	0.284	2.74	d	54.	0.88	0.284	2.01	d
73.6	1.25	0.556	2.46	d	45.	0.80	0.556	1.73	d
59.	1.12	0.899	2.12	d	33.	0.69	0.899	1.39	d
49.	1.02	1.19	1.83	d	25.	0.60	1.19	1.10	d
42.	0.94	1.37	1.65	d	20.	0.54	1.37	0.92	d
32.	0.82	1.71	1.31	d					
22.	0.68	2.16	0.86	d					

[a] See Figs. 4 and 5. [b] Reference 13. [c] Reference 12. [d] Reference 14.
[e] This work (see Fig. 6 and 11). [f] Reference 15. [g] Reference 11.

can give an adequate fit from the initial energy to about one-half the initial energy. The value of α_i is in every case about 2/3.

There are rather large discrepancies in the energy-loss measurements for the light fragment in Au, as shown in Figs. 8 and 10. The radiochemical measurements (see Fig. 11) and those of Reference 14 were both calibrated by comparison to the energy-loss data in Al from Reference 13. The agreement is satisfactory for the heavy fragment, but rather poor for the light fragment. We consider the radiochemical measurements to be more accurate and have thus weighted them more heavily in drawing the smooth curves in Figs. 8 and 10. A smaller discrepancy also exists between the radiochemical results and the time-of-light measurements for 3.3 mg/cm^2 Au absorber. The radiochemical results indicate that the range-energy curves in Al and Au are very nearly proportional to each other for the initial part of the range.

ESTIMATION OF ENERGIES FROM RANGE MEASUREMENTS

We assume that Eqs. (16) and (17) may be generalized to all fission products. Each of these equations has two parameters. We have estimated one parameter from the range-energy curves for the median light and heavy products. The other parameter was determined from the total range and the initial energy measurements. The values of k_i were assumed to be linear functions of mass and were interpolated from the median light and heavy product. Then, the Δ_i values were calculated from the ranges in Fig. 4 and the initial energies.[12] Similarly, α_i was taken to be 2/3 in every case and k_i was calculated. The parameters are shown as a function of mass in Figs. 12-14. If we assume that these parameters are smooth functions of mass we can extrapolate to the regions of low yields.

Thus from the range measurements for Ag^{111}, Cd^{115}, Br^{83}, In^{117}, and Eu^{157} we can estimate energies. Energy estimates from the two functional forms (Eqs. (16) and (17)) agree to about 0.5 Mev except for Br^{83} in fission of Pu^{239}. A kinetic energy of 105 Mev was estimated from Eq. (17) and 110 Mev from Eq. (16).

The energies are shown in Fig. 15 as a function of mass for fission of U^{235} and Pu^{239}. For U^{235} and Pu^{239} fission the total kinetic energies of the symmetric products are less than those of the slightly asymmetric products by about 30 and 20 Mev respectively. This effect may be the result of an irregularity in the range-energy parameters, but we consider it unlikely that there is an irregularity of this magnitude. This kinetic-energy deficit must be made up by unusually high excitation energies for the symmetric fragments or by the emission of particles or photons at the instant of fission. Additional experimental information is needed to distinguish between these possible alternatives.

ACKNOWLEDGMENTS

The authors are grateful for a number of suggestions and criticisms from Dr. Lester Winsberg, Dr. Wladyslaw Swiatecki, Professor N. Sugarman, Dr. Earl Hyde, and Dr. Paul Benioff.

We are grateful to Dr. Eugene Huffman, Edward Jeung, Ursula Abed, and David Sisson for many chemical analyses, to Dan O'Connell for the preparation of Au foils by evaporation techniques, and to Dr. Torbjørn Sikkeland for assistance in the preparation of the U^{235} target layers.

REFERENCES

1. E. M. Douthett and D. H. Templeton, Phys. Rev. 94, 128 (1954).
2. Nathan Sugarman, Milton Compos and Karoline Wielgoz, Phys. Rev. 101, 388 (1956).
3. Norbert T. Porile and Nathan Sugarman, Phys. Rev. 107, 1410 (1957).
   Norbert T. Porile, Phys. Rev. 108, 1526 (1957).
4. Christiane Baltzinger, "Yield and Range Studies of Selected Fission Products from Uranium Bombarded with Bev Protons", Lawrence Radiation Laboratory Report UCRL-8430, 1959.
5. Cohen, Jones, McCormick, and Ferrell, Phys. Rev. 94, 625 (1954).
6. Cohen, Ferrell-Bryan, Coombe, and Hullings, Phys. Rev. 98, 685 (1955).
7. E. J. Winhold and I. Halpern, Phys. Rev. 103, 990 (1956).
8. C. T. Coffin and I. Halpern, Phys. Rev. 112, 536 (1958).
9. J. W. Meadows, Phys. Rev. 110, 1109 (1958).
10. R. Wolke and J. Gutmann, Phys. Rev. 107, 850 (1957).
11. Katcoff, Miskel, and Stanley, Phys. Rev. 74, 631 (1948).
12. William E. Stein, Phys. Rev. 108, 94 (1957).
13. R. B. Leachman and H. W. Schmitt, Phys. Rev. 96, 1366 (1954).
14. Clyde B. Fulmer, Phys. Rev. 108, 1113 (1957), and "Fission Fragment Studies by Magnetic Analysis", Oak Ridge National Laboratory Report ORNL-2320, August, 1957.
15. P. F. Suzor, Ann. Phys. 4, 269 (1949).
16. Finkle, Hoagland, Katcoff, and Sugarman, Radio-Chemical Studies: The Fission Products, Paper No. 46, in National Nuclear Energy Series Plutonium Project Record, Vol. 9, Div. IV (McGraw-Hill Book Company, Inc., New York, 1951), p. 471.

17. Lester Winsberg, in Chemistry Division Semiannual Report, Lawrence Radiation Laboratory Report UCRL-8618, Feb. 1959, p. 44.

18. Albert Ghiorso and Torbjørn Sikkeland, in Proceedings of the Second United Nations International Conference on the Peaceful Uses of Atomic Energy, Geneva, 1958, Vol. 14 (United Nations, New York, 1959), P/2440, p. 158.

19. Radio-Chemical Studies: The Fission Products, National Nuclear Energy Series Plutonium Project Record, Vol. 9, Div. IV. (McGraw-Hill Book Company, Inc., New York, 1959).

20. N. Bohr, Kgl. Danske Videnskab. Selskab. Math.-fys. Medd. 18, No. 8 (1948).

21. Luis Muga (Lawrence Radiation Laboratory), private communication, 1959.

22. Bøggild, Arrøe and Sigurgeirsson, Phys. Rev. 71, 281 (1947).

23. Lester Winsberg and J. M. Alexander, "The Stopping of Heavy Atoms", Lawrence Radiation Laboratory report UCRL-8997, in preparation.

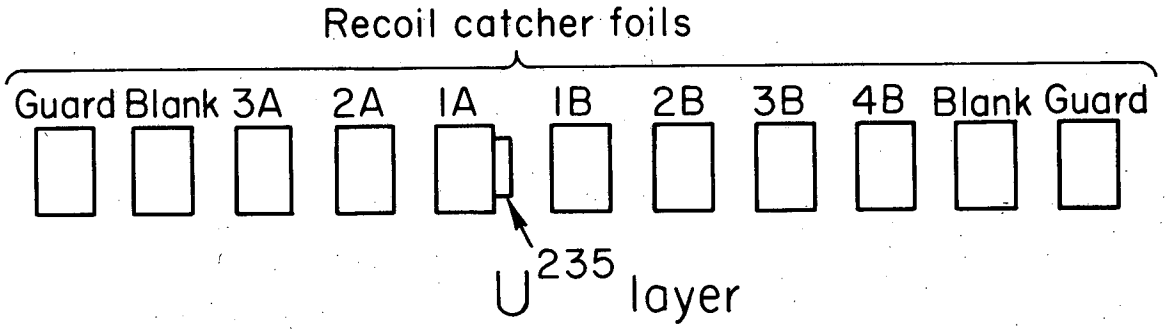

MU – 18683

Fig. 1. Diagram of the foil stack. A thin layer of fissile material was supported on the surface of catcher 1A. Space between the foils is only for clarity of the drawing; during the irradiation the foils were in contact.

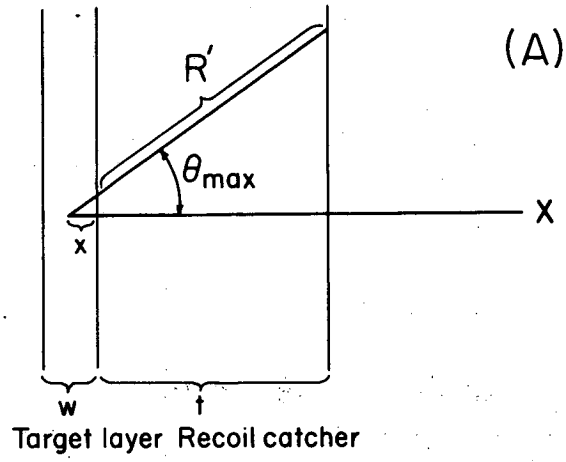

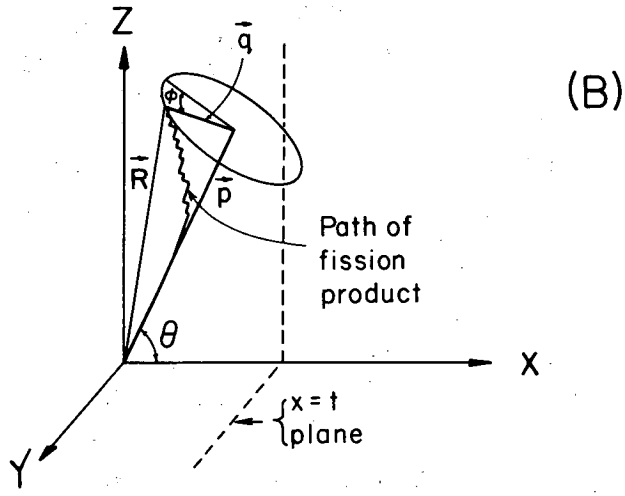

MU-18694

Fig. 2. Vector diagram of the recoiling fission product. The X axis is chosen to be normal to the surface of the target layer. The X=t plane represents the interface between catcher 1 and catcher 2. If all catcher foils are of the same material, scattering phenomena need not be considered and the upper diagram (A) is appropriate [see Eqs. (1) and (2)].

The lower diagram (B) indicates the recoil path of a particular product from an infinitely thin fissile layer in the YZ plane. The Z axis is chosen to be in the plane defined by the X axis and the initial recoil direction $\vec{p}$. The angle Φ is defined by the XZ plane and the component of the range $\vec{q}$ perpendicular to the original recoil path.

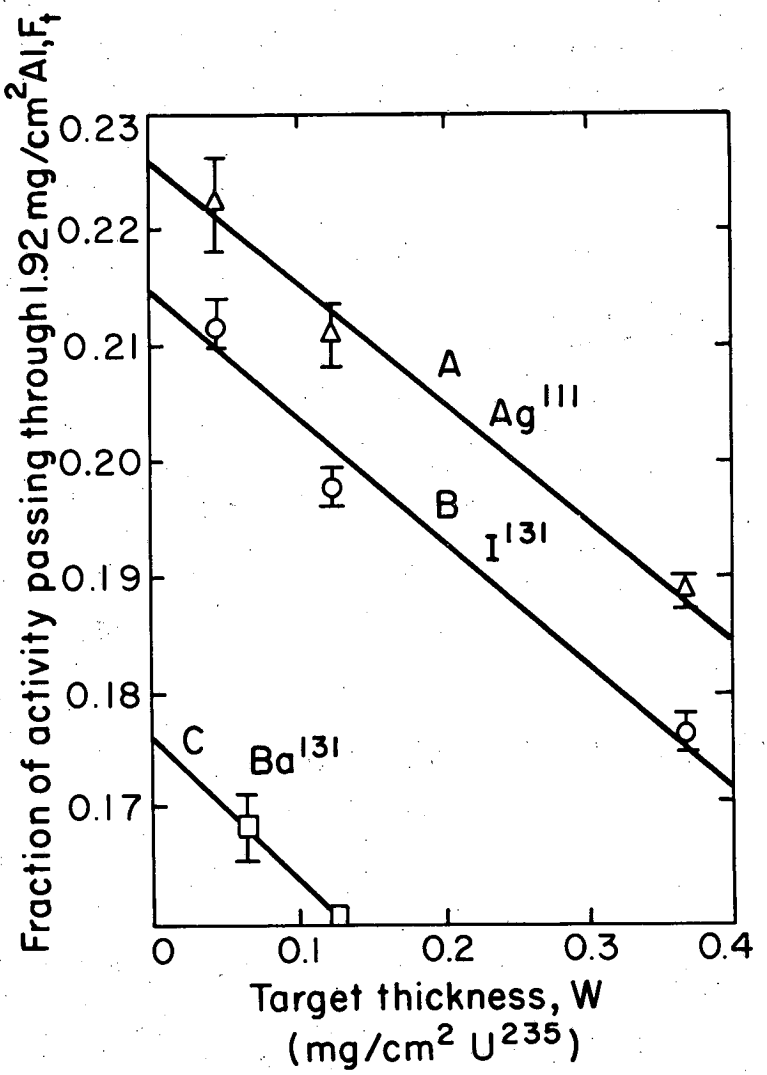

Fig. 3. Least-squares fit to linear dependence of F_t on W. The ratio (k_{Al}/k_W) of initial rate of velocity loss in the target to that in Al was determined for Ag^{111}, I^{131}, and Ba^{140}.

A: Ag^{111}: k_{Al}/k_W = 1.48 (least squares)
B: I^{131}: k_{Al}/k_W = 1.45 (least squares)
C: Ba^{140}: k_{Al}/k_W = 1.49

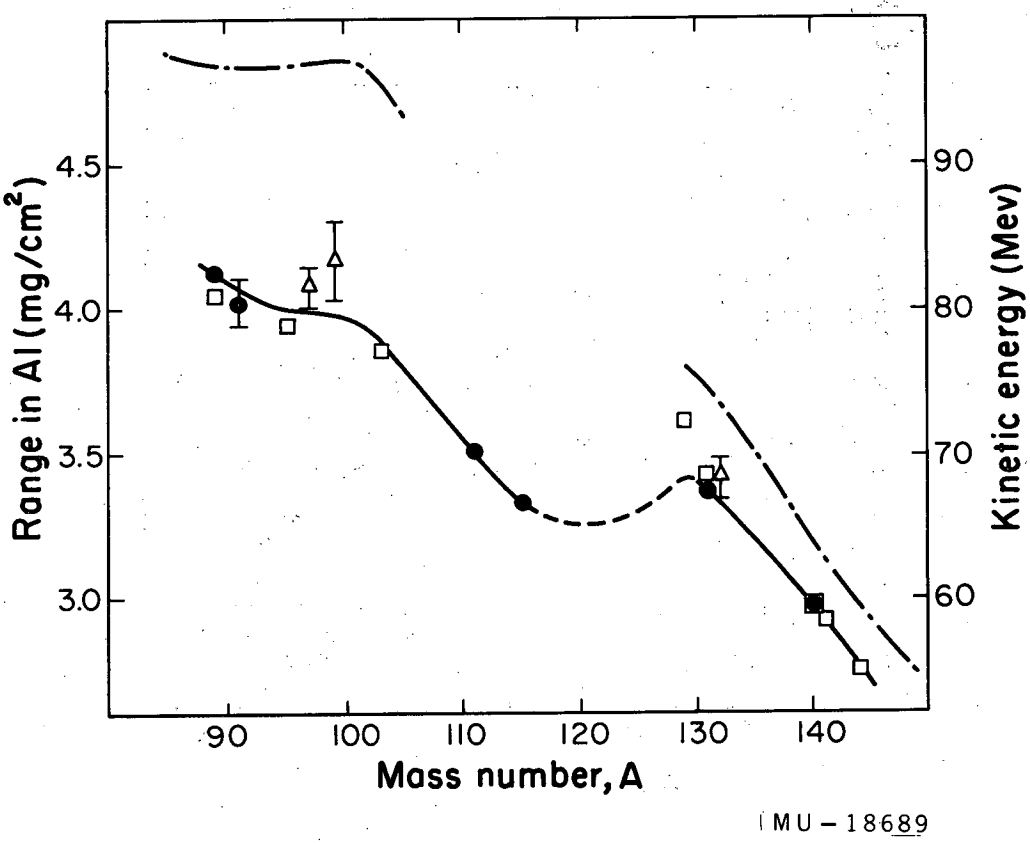

Fig. 4. Range in Al and kinetic energy of products from fission of U^{235} induced by thermal neutron irradiation. The experimental range values are designated as follows: The circles from this work; The triangles from reference 15; and the squares from reference 16, normalized to these results by the factor 1.084. The dot-and-dash curve shows the kinetic energy of the products as taken from reference 12.

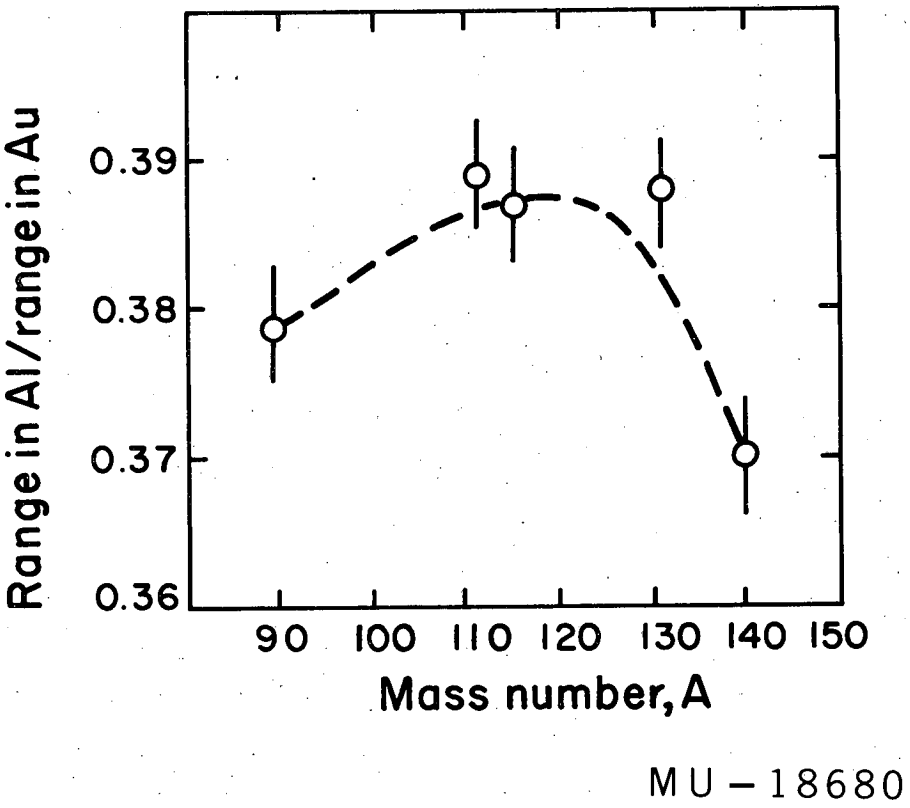

Fig. 5. The ratio of range in Al to range in Au. The limits of error for the range in Au are not well known but are believed to be about 2%.

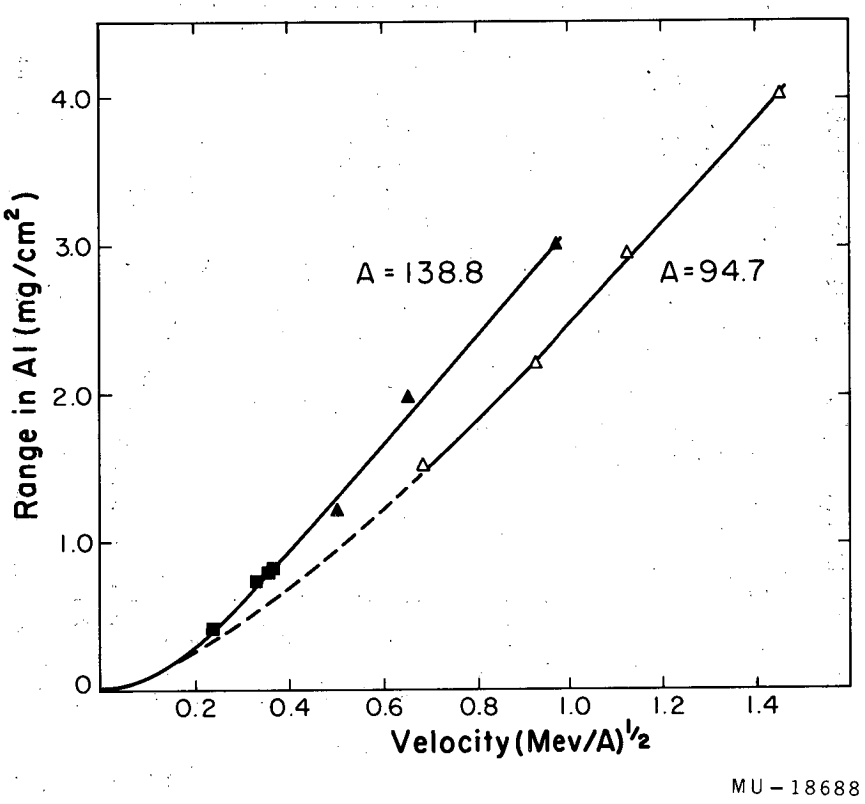

Fig. 6. Range-velocity curve in Al for the median light (open points) and heavy (closed points) fission products. The triangles are from the range measurements of this work and the energy measurements of reference 13. The squares are from the measured range of Tb^{149} recoils (formed in nuclear reactions, reference 23) converted to the median heavy fragment of the same velocity.

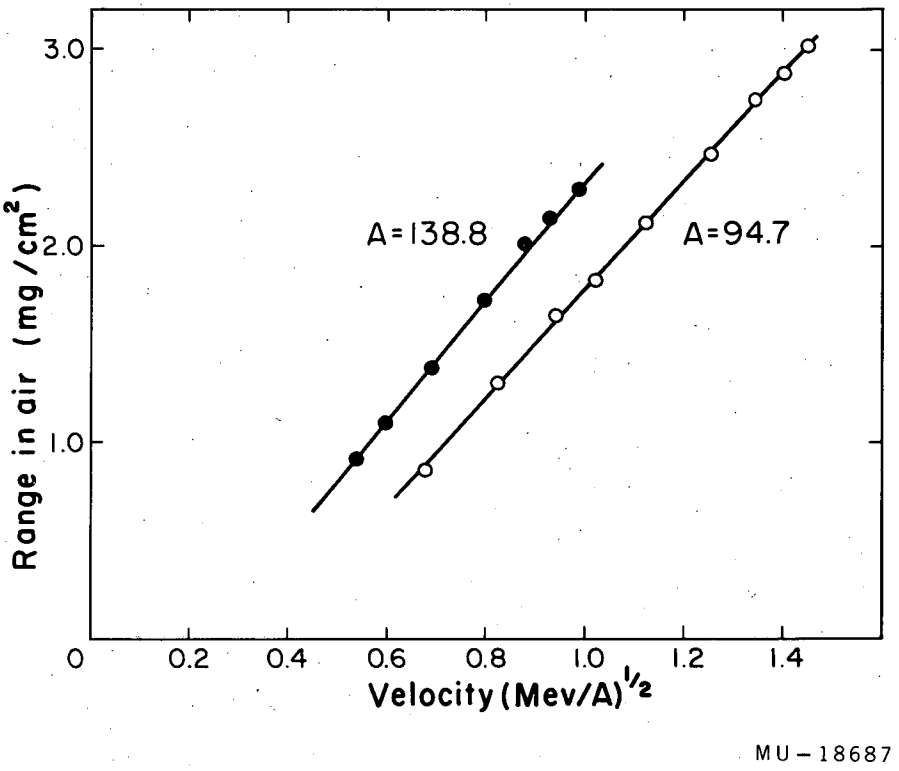

Fig. 7. Range-velocity curves in air for the median light (open points) and heavy (closed points) fission products. Total range measurements are from reference 11 and the energy measurements are from reference 14.

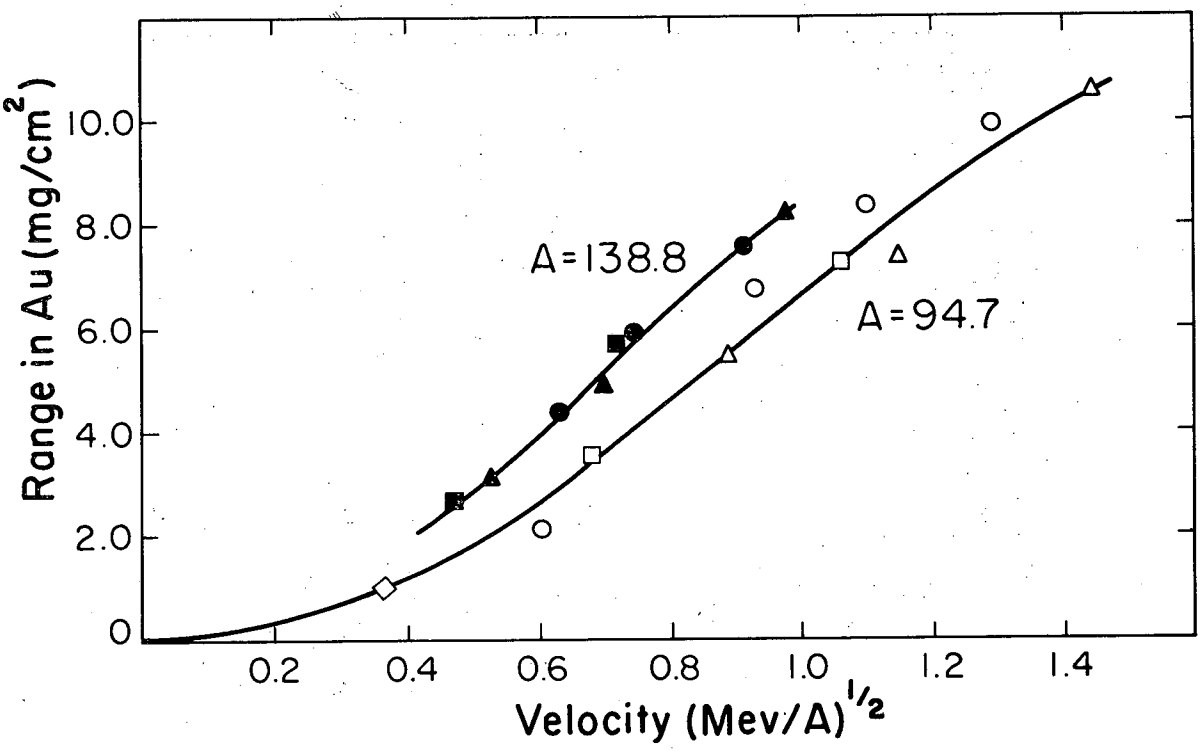

MU-18690

Fig. 8. Range-velocity curves in Au for the median light (open points) and heavy (closed points) fission products. The squares are from this work and Fig. 6, the triangles from reference 13, the circles from reference 14, and the diamond from reference 15 and Fig. 6.

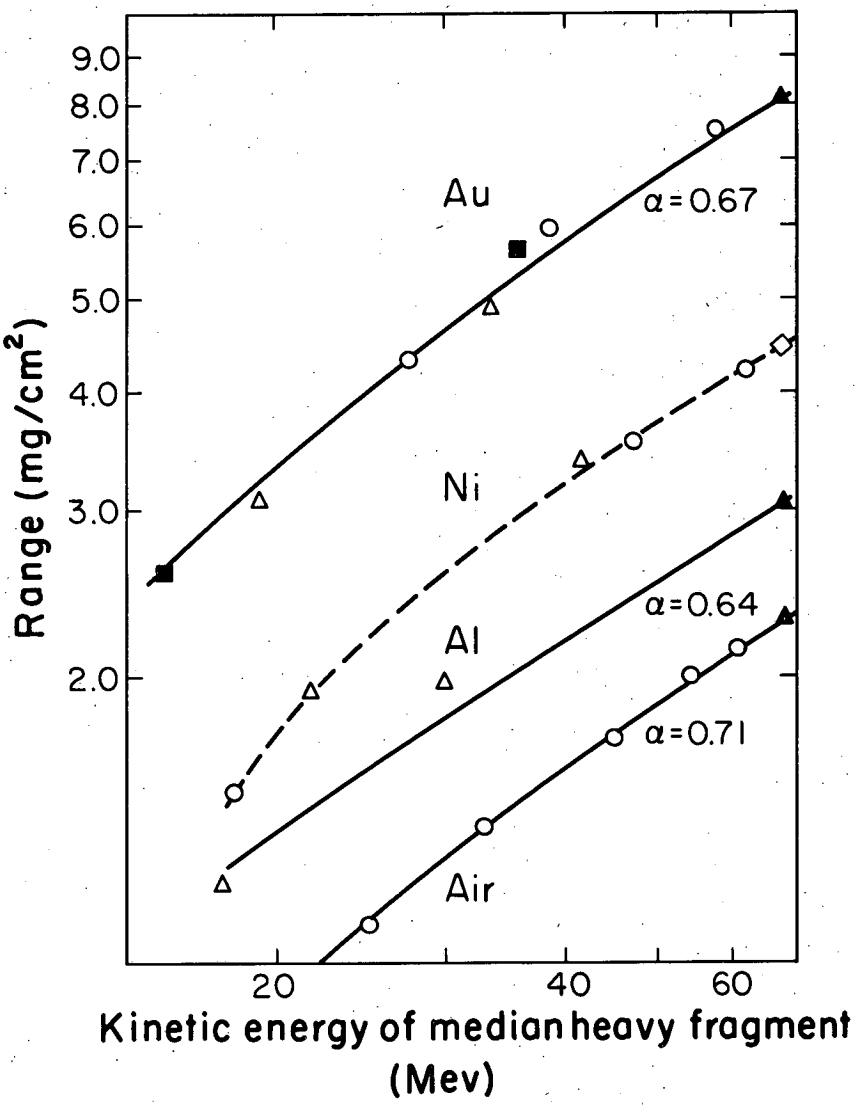

MU-18693

Fig. 9. Range-energy curves for the median heavy fission product. The smooth curves were drawn by eye to indicate that a function of the form $R_i = K_i E^{\alpha_i}$ gives an adequate fit for the initial part of the range. Closed points are from radiochemical measurements of the range. Open circles are from reference 14; triangles are from reference 13. The total range in Ni (diamond) was estimated in a crude way as described in the text. Thus the range-energy curve in Ni (dashed line) should be taken as only a rough approximation.

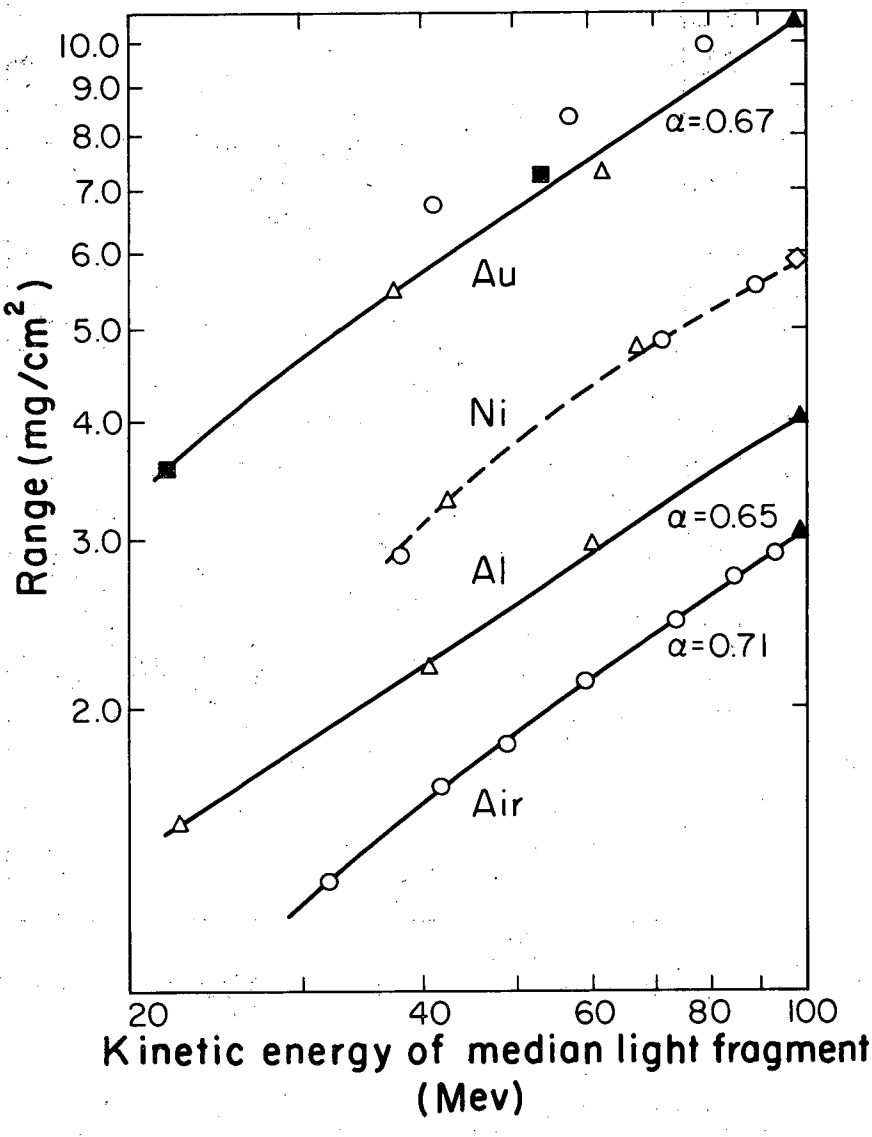

MU-18691

Fig. 10. Range-energy curves for the median light fission product. The smooth curves were drawn by eye to indicate that a function of the form $R_i = K_i E^{\alpha_i}$ gives an adequate fit for the initial part of the range. Closed points are from radiochemical measurements of the range. Open circles are from reference 14; triangles are from reference 13. The total range in Ni (diamond) was estimated in a crude way as described in the text. Thus the range-energy curve in Ni (dashed line) should be taken as only a rough approximation.

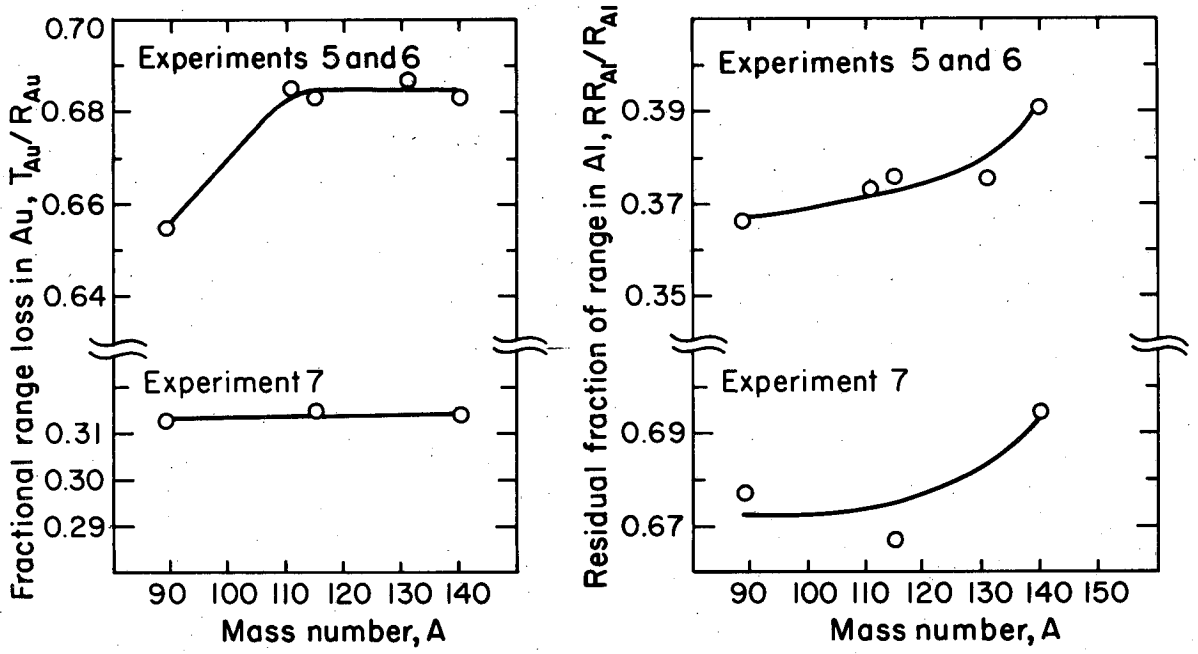

MU-18681

Fig. 11. Fractional range loss in Au (T_{Au}/R_{Au}) and fractional residual range in Al (RR_{Al}/R_{Al}). If these two fractions sum to unity the range-energy curve in Al is proportional to the range-energy curve in Au, for the particular values of T_{Au} and RR_{Al}.

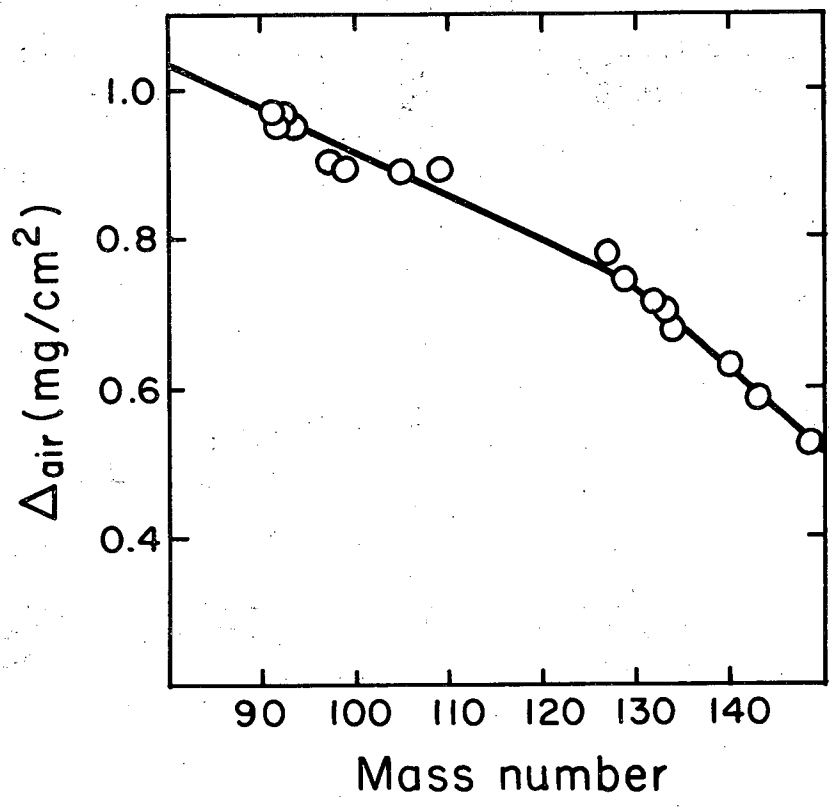

MU-18685

Fig. 12. The constant Δ_{air} in the relation $R_{air} = k_{air} V^{-\Delta_{air}}$ calculated from the initial energy (reference 12) and the total range (reference 11). The value of k_{air} was taken to be 5.44×10^{-3} A+2.253 [velocity in units of $(\text{Mev/A})^{1/2}$ and range in mg/cm^2 air].

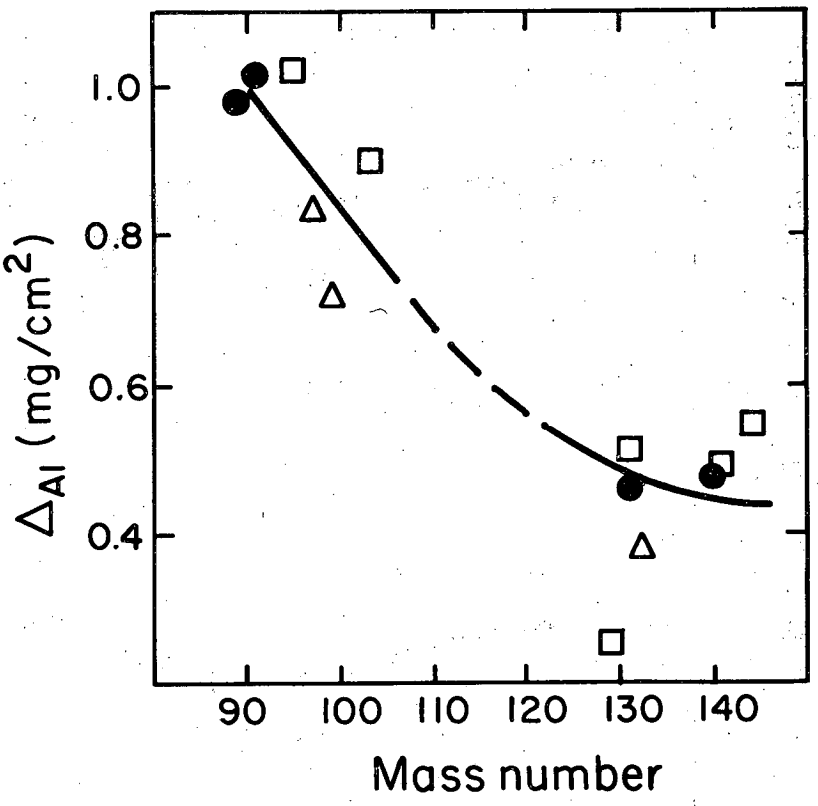

MU-18684

Fig. 13. The constant Δ_{Al} in the relation $R_{Al} = k_{Al} V - \Delta_{Al}$ calculated from the initial energy (reference 12) and the total range. The value of k_{Al} was taken to be 2.84×10^{-3} A+3.206 [velocity in units of $(\text{Mev/A})^{1/2}$ and range in mg/cm^2 Al]. The range values came from this work (closed circles), reference 15 (triangles), and reference 16 normalized to this work (squares).

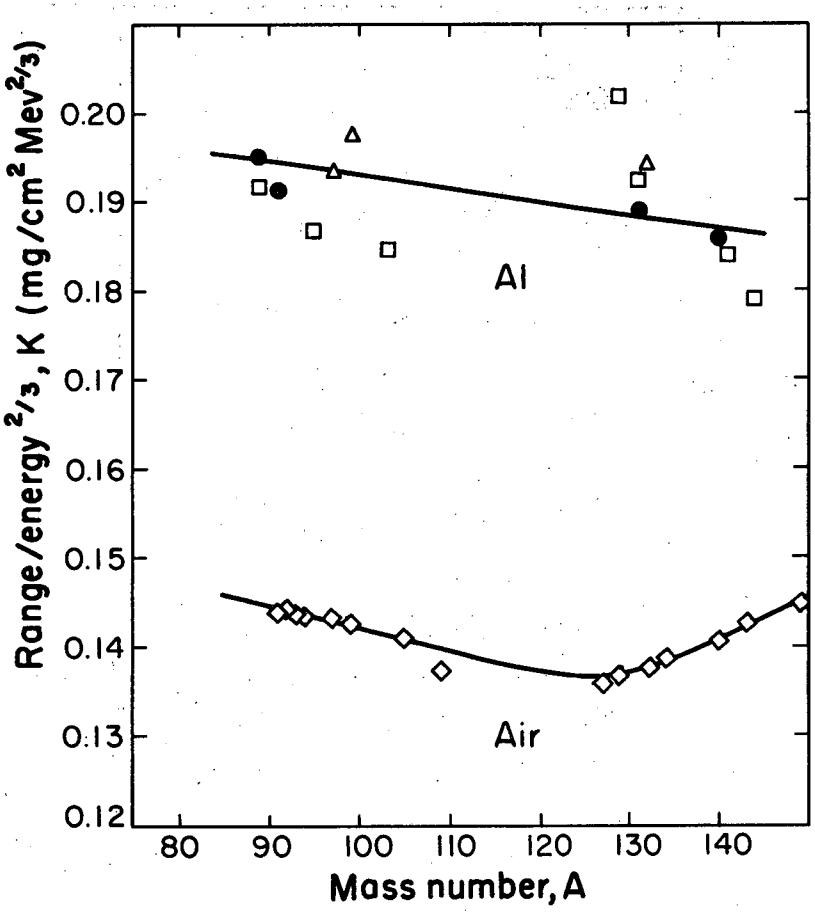

Fig. 14. The constant K in the relation $R_i = K_i E^{2/3}$, calculated from the initial energy in Mev (reference 12) and the total range (in mg/cm^2). Closed circles are from range data of this work, squares reference 16, triangles reference 15, diamonds reference 11.

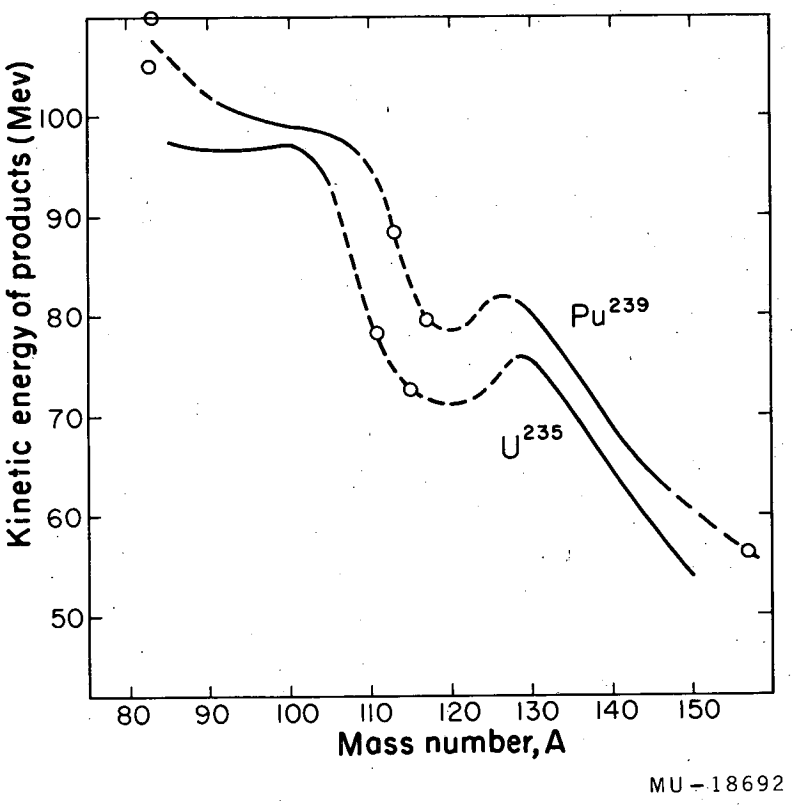

Fig. 15. The energy of the fission products. The solid curves are taken from reference 12. The circles were obtained from range measurements and extrapolated range-energy parameters.